DALTON
FULL PAPER

The *trans* effect and *trans* influence of triphenyl arsine in platinum(II) complexes. A comparative mechanistic and structural study †

Nikodem Kuznik [a,b] **and Ola F. Wendt** *[a]

[a] *Inorganic Chemistry, Department of Chemistry, Lund University, P.O. Box 124, S-221 00 Lund, Sweden. E-mail: ola.wendt@inorg.lu.se*
[b] *Chemistry Department, Silesian University of Technology, Krzywoustego 6, 44-101 Gliwice, Poland*

Received 27th February 2002, Accepted 5th June 2002
First published as an Advance Article on the web 9th July 2002

The kinetics and mechanism of the reaction between $[PtI_3(AsPh_3)]^-$ and pyridine in acetonitrile solvent has been studied by use of stopped-flow spectrophotometry. Substitution of iodide *trans* to arsine is irreversible under the conditions used and takes place *via* parallel direct and solvolytic pathways. By comparing the rate constants of the direct pathway with literature values of the corresponding phosphine and stibine complexes the following *trans* effect series can be obtained: $Ph_3Sb > Ph_3P > Ph_3As$. The crystal and molecular structures of reactant and product have been determined. Based on Pt–I distances for the investigated arsine complex and literature data for the corresponding phosphine and stibine complexes the following *trans* influence series was derived: $Ph_3P \geq Ph_3As > Ph_3Sb$. To the best of our knowledge this is the first comparison of all the three heavier pnictogens as donor atoms using strictly analogous complexes with identical *cis*-ligands.

Introduction

Pnictogen donor ligands and especially phosphines are ubiquitous in the coordination and organometallic chemistry of platinum(II).[1] However, the number of complexes investigated become more scarce as you proceed down Group 15. There are a few examples of crystal structures of stibine complexes of the platinum group metals, and crystal structures of platinum(II) stibine complexes were only recently published.[2–4] *trans* Influences and *trans* effects and their origin continue to intrigue chemists and is still an active area of research.[5] To probe the *trans* effect of different ligands the reactions of heterocyclic amines and other nucleophiles with complexes of the type $[PtCl_3(L)]^-$ have been investigated for neutral ligands L.[6] Previous work has also aimed at subdividing the *trans* effect into its σ- and π-components by means of an analysis of the nucleophilic discrimination. To our knowledge there is still no strictly analogous series of complexes with the heavier pnictogen donor atoms (P, As, Sb) that has been investigated with respect to structure and reactivity in this sense and where the only factor being changed is the nature of the *trans* donor. We therefore thought it timely to complete our earlier investigation on $[PtI_3(EPh_3)]^-$ (E = P, Sb) complexes with data on the corresponding arsine complex.[3b] Here we report on the kinetics and mechanism for the reaction of $[PtI_3(AsPh_3)]^-$ with pyridine together with the crystal structures of $(Bu_4N)[PtI_3(AsPh_3)]$ and $[PtI_2(py)(AsPh_3)]$.

Experimental

General procedures and materials

$(Bu_4N)_2[Pt_2I_6]$ was prepared according to the literature.[7] Pyridine was refluxed over KOH pellets and distilled prior to use. All other reagents and solvents were purchased and used without further purification. Elemental analysis was performed by Mikro Kemi AB, Uppsala, Sweden. NMR spectra were recorded on a Varian Unity 300 spectrometer. Chemical shifts are given in ppm downfield from TMS using residual solvent peaks as internal standard.

Synthesis

$(Bu_4N)[PtI_3(AsPh_3)]$([Bu_4N][1]). A sample of $(Bu_4N)_2[Pt_2I_6]$ (0.191 g, 0.117 mmol) was dissolved in 10 cm^3 CH_2Cl_2. A solution of $AsPh_3$ (0.069 g, 0.225 mmol) in 15 cm^3 CH_2Cl_2 was added dropwise and the resulting solution was stirred at room temperature overnight. The solvent was evaporated and the crude product recrystallised from CH_2Cl_2–diethyl ether (1 : 1) yielding 0.209 g (83%) of **1**. Anal. calc. for $C_{34}H_{51}AsI_3NPt$: C 36.3; H 4.6. Found: C 36.6; H 4.6%. ^{1}H NMR ($CDCl_3$, 299.79 MHz): δ 1.02 (t, J = 7.3 Hz, 12H), 1.44–1.55 (m, 8H), 1.63–1.76 (m, 8H), 3.31–3.41 (m, 8H), 7.30–7.45 (m, 9H), 7.63–7.80 (m, 6H).

***trans*-[$PtI_2(AsPh_3)(py)$] (2).** A sample of [Bu_4N][**1**] (23.7 mg, 0.021 mmol) was dissolved in 10 cm^3 MeCN. Pyridine (py, 0.017 cm^3) was added and the solution was stirred for 1 h. The solvent was evaporated to 1/3 of the original volume and the solution was kept in a freezer overnight. The solution was decanted and the orange crystals formed were washed twice with cold MeCN and dried *in vacuo*. Yield: 8 mg (46%). Anal. calc. for $C_{23}H_{20}AsI_2NPt$: C 33.1; H 2.4. Found: C 32.9; H 2.6%. ^{1}H NMR ($CDCl_3$, 299.79 MHz): δ 7.34–7.36 (m, 12 H), 7.72–7.78 (m, 6 H), 9.03–9.07 (m, 2 H, $^3J_{Pt-H}$ = 36 Hz, *o*-H).

Structure determination

Single crystals of [Bu_4N][**1**] and **2** suitable for X-ray diffraction were obtained by slow evaporation at room temperature of the solvent from a dichloromethane–hexane solution (*ca.* 1 : 1) of [Bu_4N][**1**] and an acetonitrile solution of complex **2**.

Crystal data and data collection details are given in Table 1. The intensity data sets for [Bu_4N][**1**] and **2** were collected at

† Electronic supplementary information (ESI) available: observed pseudo-first order rate constants for reaction (4) in acetonitrile at different temperatures and ligand concentrations. Equilibrium absorbances for the solvolysis of complex **1** and **2** at 25 °C in acetonitrile at different iodide and pyridine concentrations, respectively. See http://www.rsc.org/suppdata/dt/b2/b202100p/

 DOI: 10.1039/b202100p

Table 1 Details of data collection and refinement

Compound	[Bu_4N][**1**]	**2**
Chemical formula	$C_{34}H_{51}AsI_3NPt$	$C_{23}H_{20}AsI_2NPt$
MW/g mol^{-1}	1124.5	834.21
Crystal system	Monoclinic	Monoclinic
Space group	$P2_1/n$	$P2_1/n$
a/Å	9.788(2)	12.869(3)
b/Å	18.474(4)	11.283(2)
c/Å	21.956(4)	16.842(3)
β/°	98.67(3)	101.83(3)
V/Å^3	3925(2)	2393.6(8)
Z	4	4
μ/mm^{-1}	6.79	9.822
Collected reflections	38886	23939
Unique reflections	12004 (R_{int} = 0.0906)	7407 (R_{int} = 0.0672)
No. of parameters	361	253
$R(F)$, $wR(F^2)$ ($I > 2\sigma(I)$)	0.0453, 0.0939	0.0481, 0.1128
$wR(F^2)$ (all data)	0.1178	0.1302
S	0.939	0.944

293 K with a Bruker SMART CCD system with a rotating anode (Mo-Kα radiation, λ = 0.71073 Å) using ω-scans.[8] The intensities were corrected for Lorentz, polarisation and absorption effects using SADABS.[9] In both data sets the first 50 frames were collected again at the end to check for decay and none was observed. All reflections were integrated using SAINT.[10] Both structures were solved by Patterson methods and refined by full-matrix least-squares calculations on F^2 using SHELXTL5.1.[11] Non-H atoms were refined with anisotropic displacement parameters. Hydrogen atoms were constrained to parent sites, using a riding model.

Both models contain residual peaks with $\Delta\rho > 1$ e Å^{-3}, but they are situated less than 1.15 Å from an iodide or platinum atom.

CCDC reference numbers 180736 and 180737.

See http://www.rsc.org/suppdata/dt/b2/b202100p/ for crystallographic data in CIF or other electronic format.

Kinetics

The stopped-flow experiments were performed on an Applied Photophysics Bio Sequential SX-17 MX, stopped-flow spectrofluorimeter. The substitution of iodide in **1** by pyridine was studied in acetonitrile solvent by observing the decrease in absorbance at 366 nm. The complex solution (5× 10^{-5} mol dm^{-3}) containing excess iodide (5–20 × 10^{-3} mol dm^{-3}) was mixed directly in the stopped-flow instrument with an equal volume of pyridine solution, resulting in a large excess of entering ligand (1–10 × 10^{-2} mol dm^{-3}), assuring pseudo first-order conditions. The kinetic traces were fitted to single exponentials using the software provided by Applied Photophysics,[12] resulting in observed rate constants at different concentrations of leaving and incoming ligand. Rate constants are given as an average of at least five runs. Time-resolved spectra were also recorded on the Applied Photophysics instruments. Variable-temperature experiments were performed between 288 and 318 K. Complete data are reported in ESI Table S1.

UV/VIS equilibrium measurements

UV/VIS spectra were recorded on a Milton Roy 3000 diode array spectrophotometer. The equilibrium absorbance in the solvolysis of **1** and **2** according to reaction (1) below was measured for different [I$^-$] and [py], respectively. Complete data are reported in ESI Table S2.

Results

Synthesis

Mixed platinum arsine complexes have earlier been prepared by cleaving the dinuclear [PtCl(AsR_3)(μ-Cl)]$_2$ with neutral solvents or two-electron donors.[6d,13] This method is sometimes inconvenient due to the decreasing thermal stability of the dinuclear complexes going down Group 15 and the general difficulties in preparing and purifying them. Instead, using a procedure that was earlier used for the analogous phosphine and stibine complexes,[3b] the $[Pt_2I_6]^{2-}$ ion was cleaved by use of a stoichiometric amount of $AsPh_3$ giving **1** as the only product in high yield. Compound **2** was made from **1** with an excess of pyridine.

Crystal structures

The anionic complex **1** is isostructural with the corresponding phosphine and stibine analogues.[3b] Its structure is given in Fig. 1. The molecular structure of **2** is given in Fig. 2. In both cases

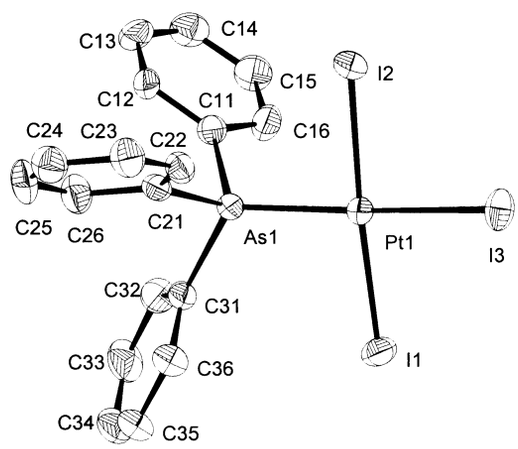

Fig. 1 Diamond drawing with atomic numbering of the structure of the anionic complex **1**. The ellipsoids denote 30% probability. The tetrabutylammonium cation was omitted for clarity.

the coordination geometry around platinum is distorted square-planar with angles ranging from 87.8 to 93.6° in **1** and from 87.9 to 92.6° in **2**. The largest deviations from a least-squares plane through PtI_2XAs is 0.14 Å (I1 and I2) in **1** (X = I) and 0.057 Å (I1 and I2) in **2** (X = N). The plane of the pyridine is almost perpendicular (72.9°) to the coordination plane. Selected bond distances and angles are given in Table 2.

Solvolysis

The UV/VIS spectrum of **1** dissolved in MeCN changes when free iodide is added and one peak in the visible region at 363 nm grows in. The spectral changes are best explained by a solvolytic equilibrium according to eqn. (1).

Table 2 Selected crystallographic distances (Å) and angles (°) with estimated standard deviations

	1 (X = I3)	**2** (X = N1)
Pt1–I1	2.6112(9)	2.5855(8)
Pt1–I2	2.6181(9)	2.6062(8)
Pt1–X	2.6585(7)	2.109(5)
Pt1–As1	2.3753(8)	2.3567(8)
As1–C11	1.965(7)	1.946(6)
As1–C21	1.954(7)	1.935(7)
As1–C31	1.964(6)	1.941(6)
I1–Pt1–X	90.27(2)	87.94(16)
I2–Pt1–X	88.96(2)	88.34(16)
I1–Pt1–As1	93.60(2)	92.60(4)
I2–Pt1–As1	87.79(2)	91.15(4)
C11–As1–C21	106.8(3)	107.1(3)
C11–As1–C31	100.6(3)	100.3(3)
C21–As1–C31	99.7(3)	102.2(3)

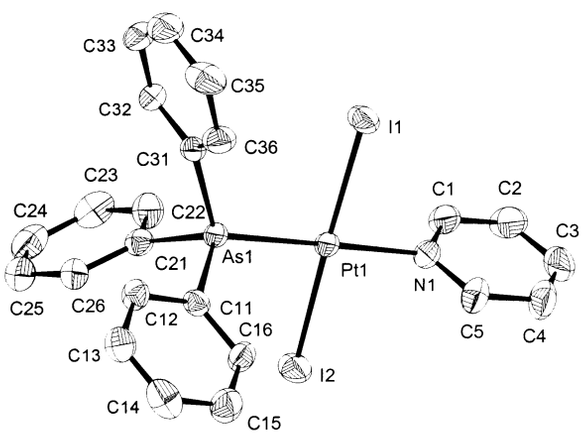

Fig. 2 Diamond drawing with atomic numbering of the molecular structure of complex **2**. The ellipsoids denote 30% probability.

$$[PtI_3(AsPh_3)]^- + MeCN \underset{}{\overset{K_1}{\rightleftharpoons}} \underset{\mathbf{3}}{trans\text{-}[PtI_2(AsPh_3)(MeCN)]} + I^- \quad (1)$$
$$\mathbf{1}$$

This is a fairly fast equilibrium (after a few minutes there are no spectral changes with time) and its equilibrium constant, K_1, was determined by measuring the absorbance at different iodide concentrations. Eqn. (2), where A_∞ (the absorbance at infinite $[I^-]$), ε_M (the extinction coefficient of **3** at the path length used) and K_1 are the adjustable parameters, was fitted to the data.

$$A = \frac{A_\infty[I^-] + \varepsilon_m K_1[Pt]}{K_1 + [I^-]} \quad (2)$$

The fit (Fig. 3) gave $K_1 = (3.4 \pm 0.4) \times 10^{-3}$ mol dm^{-3}.

The initial UV/VIS spectrum of **2** in MeCN changes substantially upon addition of pyridine with the largest absorbance changes at 296 and 371 nm. This suggests a similar solvolytic equilibrium, although complex **2** is less prone to solvolysis:

$$\underset{\mathbf{2}}{trans\text{-}[PtI_2(AsPh_3)(py)]} + MeCN \underset{}{\overset{K_3}{\rightleftharpoons}} \underset{\mathbf{3}}{trans\text{-}[PtI_2(AsPh_3)(MeCN)]} + py \quad (3)$$

As described above, eqn. (2) was fitted to the data at the two different wavelengths giving $K_3 = (2.6 \pm 0.5) \times 10^{-4}$ mol dm^{-3}.

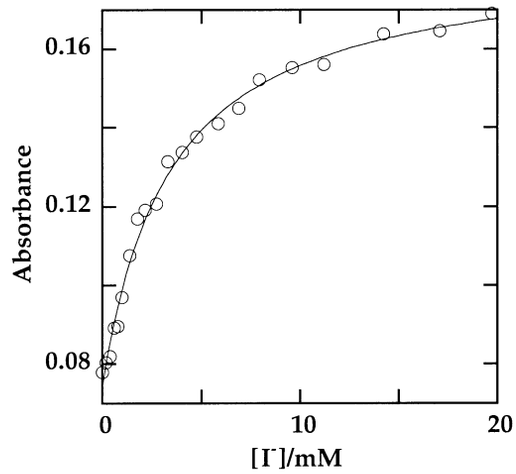

Fig. 3 Equilibrium absorbance at 363 nm for the solvolytic reaction (1) as a function of iodide concentration. T = 298.2 K. [Pt] = 1 × 10^{-4} mol dm^{-3}.

Reaction with pyridine

Reaction (4) was studied in MeCN:

$$\underset{\mathbf{1}}{[PtI_3(AsPh_3)]^-} + py \underset{}{\overset{K_2}{\rightleftharpoons}} \underset{\mathbf{2}}{trans\text{-}[PtI_2(AsPh_3)(py)]} + I^- \quad (4)$$

Time-resolved spectra of the reaction are given in Fig. 4, showing the presence of an isosbestic point at 338 nm.

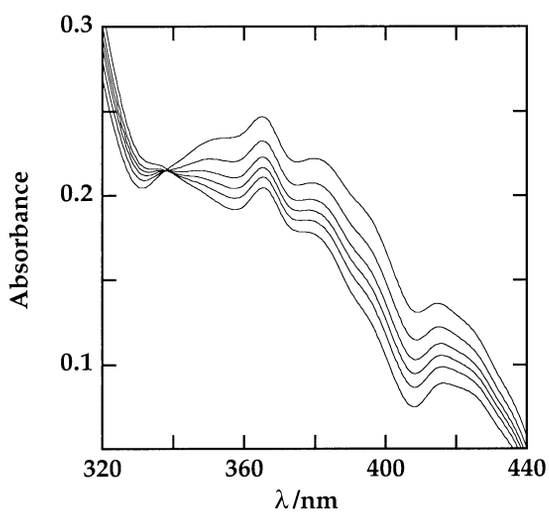

Fig. 4 Time-resolved spectra for reaction (4). T = 298.8 K. [Pt] = 5 × 10^{-5} mol dm^{-3}, [py] = 0.100 mol dm^{-3}, [I$^-$] = 5 × 10^{-3} mol dm^{-3}. Scans obtained at 1.2, 3.6, 6.0, 8.4, 12 and 36 s.

Reaction (4) is an equilibrium reaction with an approximate equilibrium constant (as determined from the ratio of solvolysis constants) of 13. During the kinetic experiments high iodide and pyridine concentrations ([py] ≥ [I$^-$] > 100[Pt]) were used to avoid solvolysis and shift the equilibrium to the right. Thus, there was no observable variation in absorbance amplitude with pyridine concentration, indicating that the position of the equilibrium does not change and is far to the right already at the lowest pyridine concentrations. Plots of k_{obs} *vs.* [py] at different [I$^-$] are linear with non-zero intercepts, *cf.* Fig. 5. The usual two-term rate law, eqn. (5), was fitted to the data.

$$k_{obs} = a + k_2[py] \quad (5)$$

Table 3 Rate constants and activation parameters for reaction (4) at 25 °C in acetonitrile solvent

	k (298.8 K)/M^{-1} s^{-1}	$\Delta H^{\ddagger}$/kJ mol^{-1}	$\Delta S^{\ddagger}$/J K^{-1} mol^{-1}
k_2-path	1.10 ± 0.06	43.7 ± 1.3	−98 ± 4
a-path (k_{-1})	0.012 ± 0.005	32.0 ± 1.8	−174 ± 6
$PtI_3(PPh_3)^-$ (k_2)[a]	9.2 ± 0.2	34.0 ± 0.4	−112.6 ± 1.2
$PtI_3(SbPh_3)^-$ (k_2)[a]	145 ± 10	11.6 ± 1.0	−165 ± 4

[a] Ref. 3*b*.

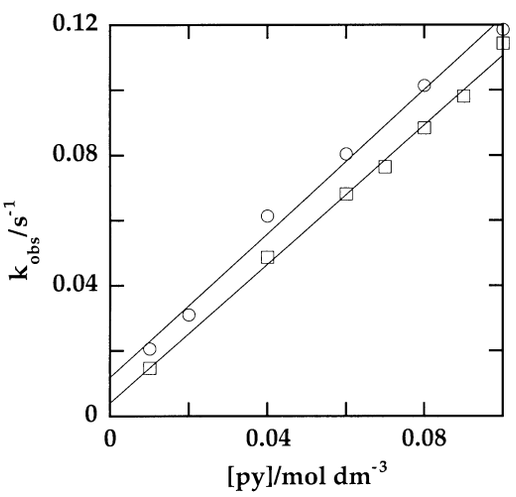

Fig. 5 Observed pseudo first-order rate constants for reaction (4) as a function of pyridine concentration at different iodide concentrations. T = 298.8 K. (○) $[I^-] = 5 \times 10^{-3}$ mol dm^{-3} (□) $[I^-] = 20 \times 10^{-3}$ mol dm^{-3}.

Activation parameters were obtained by fitting the Eyring equation to values of a and k_2 at different temperatures. Rate constants and activation parameters are given in Table 3 together with some literature values.

Discussion

Rate laws and mechanisms

Scheme 1 depicts a substitution reaction involving a solvento

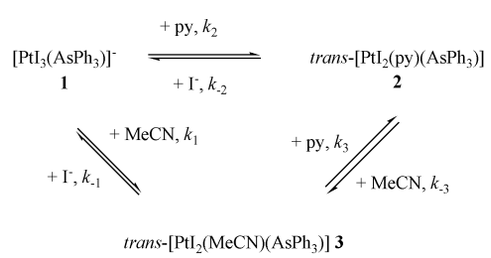

Scheme 1

species and with full reversibility in all steps. The rate law derived from this scheme, using the steady-state approximation for the solvento species, is given in eqn. (6). The use of this approximation is validated by the use of high $[I^-]$ together with the fact that Fig. 4 shows a well-defined isosbestic point, although the solvolysis constants show that **3** can exist in quite high concentrations at low nucleophile concentrations.

$$k_{obs} = k_2[py] + k_{-2}[I^-] + \frac{k_{-3}k_{-1}[I^-] + k_1k_3[py]}{k_{-1}[I^-] + k_3[py]} \qquad (6)$$

Clearly the experimental rate law (5) must be some simplification of eqn. (6). The pyridine-dependent contribution to k_{obs} in (5) can most certainly be interpreted in a direct associative attack at the metal centre (k_2-term in (6)). This is also supported by the activation parameters. The origin of the intercept is somewhat less clear. One possible explanation is a reversible reaction (k_{-2}) but this can be ruled out on the grounds that the intercept seems to decrease rather than increase with increasing iodide concentration. Also, using the value of the equilibrium constant K_2, it is obvious that the reverse reaction would give a negligible contribution to k_{obs} under the experimental conditions used. Thus the intercept arises from a parallel solvent attack at the metal centre. Usually the third term in eqn. (6) reduces to k_1. If this were the case also in the current system it would require the different intercepts in Fig. 5 to be explained by experimental error. This seems rather unlikely and probably the other rate constants in the third term of (6) also make a contribution. An attempt to fit the full expression in the rewritten form (7) gives large errors in all constants but k_2, which is not significantly altered as compared to the linear fit.

$$k_{obs} = k_2([py] + 1/K_2[I^-]) + \frac{k_2k_{-3}[py] + k_{-3}[I^-]}{[I^-] + (k_3/k_{-1})[py]} \qquad (7)$$

To conclude, the constant a can be ascribed to the solvent path, but its full mechanistic significance cannot be resolved with the current data. This also means that the activation parameters associated with this pathway should be treated with caution.

Reactivity and *trans* effect

The *trans* effect is a well established concept in platinum(II) chemistry and a lot of ligands have been investigated with respect to this property. It is generally subdivided into a σ- and a π-contribution.[14] Strong σ-donation from a ligand, giving a weaker *trans* bond (*i.e.* a high ground-state *trans* influence), increases the rate of substitution. Charge delocalization in the transition state helps to stabilise it and thus to increase the rate. Strong π-acceptors typically give this kind of stabilisation, and thus have a high *trans* effect.[15]

Complex **1** reacts with the same mechanism as the corresponding phosphine and arsine complexes. Using the k_2-values allows for the first direct comparison of the *trans* effect of the heavier pnictogens as donor atoms, *cf.* Table 3. The reactivity of the $AsPh_3$-complex is clearly lower than that of the phosphine and stibine complexes, the order of reactivity being:

$$Ph_3Sb > Ph_3P > Ph_3As$$

This is in agreement with earlier indirect comparisons and confirms the absence of a periodicity in the *trans* effects down Group 15.[3b,6d,16] The explanation is most likely a balance between σ- and π-contributions.

Before continuing this discussion it is enlightening to look at the *trans* influence sequence of the ligands. It has been proposed that the *trans* influence be used as a measure of

the σ component of the *trans* effect thus separating the two contributions.[3b] The classical way of distinguishing between these two components is to use nucleophilic discrimination as a criterion but the mechanistic ambivalence of the *a* value makes this approach uninformative.[17]

To the best of our knowledge the present results complete the first crystallographic comparison of all three heavy pnictogens and gives the following sequence of *trans* influence with the Pt–I distances in Å given in parentheses,[3b] based on Pt–I distances *trans* to PPh_3 and $SbPh_3$ of 2.662(3) and 2.637(2) Å, respectively.

$$Ph_3P\ (2.662(3)) \geq Ph_3As\ (2.6585(7)) > Ph_3Sb\ (2.637(2))$$

This is in reasonable agreement with the assessment made using NMR coupling constants which gives a monotonic decrease of *trans* influence on going down the group from phosphorus.[18] It can thus be concluded that the arsine is a stronger σ-donor than $SbPh_3$ but probably a weaker donor than PPh_3. Some results deviating from this picture have been reported but usually *cis* effects as well as packing effects cannot be ruled out in these cases. Thus, a recent crystallographic comparison using the *cis*-$PtCl_2L_2$ series have put $AsPh_3$ and $SbPh_3$ on par with each other[3a,4d] and also stibines and phosphines have been considered to have equal *trans* influences.[3g]

The lower reactivity of **1** is thus probably a ground state effect based on the lower donating ability of the arsine ligand as compared to the phosphine. In the arsine case there seems to be no significant π-stabilisation of the transition state, as is the case of the stibine having a high *trans* effect despite its inferior *trans* influence. This line of reasoning is in agreement with a recent proposal by Elding and co-workers to use the contribution of $T\Delta S^{\ddagger}$ to $\Delta G^{\ddagger}$ as a measure of how well-ordered the transition state is.[15] It seems that a high entropy contribution is associated with substitutions *trans* to ligands which derive their *trans* effect mainly from π-acidity; thus substitution *trans* to triphenylstibine has an entropy contribution at room temperature of around 80%, whereas the corresponding value for **1** is 40%, similar to what is found in the triphenylphosphine case.

To measure σ and π contributions to metal–P bonds of PR_3 complexes in the ground state also the P–C distances and C–P–C angles have been successfully used.[19,20] As shown by Orpen and co-workers[19] these two effects almost cancel for Pt–PPh_3 complexes and the average distances and angles in the complexes are approximately the same as in free PPh_3. Present data for $AsPh_3$ reveal an average As–C distance of 1.961(7) and 1.941(1) Å for **1** and **2**, respectively, to be compared with the value for free triphenylarsine of 1.957(9) Å.[21] This could be taken as further evidence for a similar σ/π ratio in the Pt–As bond as compared to the Pt–P bond. Clearly the fact that the more electron rich complex **1** has longer As–C bonds speaks in favour of the σ* orbitals being involved in π-acceptance. It has been shown earlier for all stibine complexes examined that upon coordination the Sb–C distances decrease and C–Sb–C angles increase, suggesting a different hybridisation scheme in stibine complexes.[3a,b,f,g] One explanation offered is that stibines are weaker π acceptors,[3f] but this was disputed by one of us based on the higher *trans* effect of the stibine. We instead suggest that the π acceptor function on the stibine is mainly of 5d-character.[3b]

In conclusion it therefore seems that the lower *trans* effect of arsines as compared to phosphines is explained by their lower *trans* influence, but it cannot be ruled out that the higher *trans* effect of the phosphine to some extent is due to transition state effects. On the other hand, the lower *trans* effect of arsine as compared to stibine is clearly an effect of the better π-stabilisation of the transition state that the latter exerts.

Acknowledgements

We thank Prof. Åke Oskarsson for his help with the X-ray crystallography. We are also grateful to Prof. Lars I. Elding for a generous loan of the stopped-flow instrument and for valuable discussions. Financial support from the Swedish Research Council, the Crafoord Foundation and the Royal Physiographic Society in Lund is gratefully acknowledged. N. K. thanks the Swedish Institute for a fellowship.

References and notes

1 F. R. Hartley, *The chemistry of platinum and palladium*, Applied Science Publishers, Barking, Essex, England, 1973.
2 For a review on metal stibine complexes see: N. R. Champness and W. Levason, *Coord. Chem. Rev.*, 1994, **133**, 115.
3 For crystal structures of metal-stibine complexes see: (*a*) O. F. Wendt, A. Scodinu and L. I. Elding, *Inorg. Chim. Acta*, 1998, **277**, 237; (*b*) O. F. Wendt and L. I. Elding, *J. Chem. Soc., Dalton Trans.*, 1997, 4725; (*c*) P. Sharma, A. Cabrera, M. Sharma, C. Alvarez, J. L. Arias, R. M. Gomez and S. Hernandez, *Z. Anorg. Allg. Chem.*, 2000, **626**, 2330; (*d*) M. Mathew, G. J. Palenik and C. A. McAuliffe, *Acta Crystallogr., Sect. C*, 1987, **43**, 21; (*e*) R. Cini, G. Giorgi and L. Pasquini, *Inorg. Chim. Acta*, 1992, **196**, 7; (*f*) N. J. Holmes, W. Levason and M. Webster, *J. Chem. Soc., Dalton Trans.*, 1998, 3457; (*g*) T. Even, A. R. J. Genge, A. M. Hill, N. J. Holmes, W. Levason and M. Webster, *J. Chem. Soc., Dalton Trans.*, 2000, 655; (*h*) A. Mentes, R. D. W. Kemmitt, J. Fawcett and D. R. Russell, *J. Organomet. Chem.*, 1997, **528**, 59.
4 For platinum arsine complexes see: (*a*) M. K. Cooper, P. J. Guerney and M. McPartlin, *J. Chem. Soc., Dalton Trans.*, 1980, 349; (*b*) M. H. Johansson, S. Otto, A. Roodt and Å. Oskarsson, *Acta Crystallogr., Sect. B*, 2000, **56**, 226; (*c*) S. Otto and A. J. Muller, *Acta Crystallogr., Sect. C*, 2001, **57**, 1405; (*d*) S. Otto and M. H. Johansson, *Inorg. Chim. Acta*, 2002, **329**, 135.
5 See for example: (*a*) T. G. Appleton, H. C. Clark and L. E. Manzer, *Coord. Chem. Rev.*, 1973, **10**, 335; (*b*) A. Fischer and O. F. Wendt, *J. Chem. Soc., Dalton Trans.*, 2001, 1266; (*c*) S. Otto and L. I. Elding, *J. Chem. Soc., Dalton Trans.*, 2002, 2354; (*d*) K. M. Anderson and A. G. Orpen, *Chem. Commun.*, 2001, 2682; (*e*) M. H. Johansson, Å. Oskarsson, K. Lövqvist, F. Kiriakidou and P. Kapoor, *Acta Crystallogr., Sect. C*, 2001, **57**, 1053.
6 (*a*) R. Romeo and M. L. Tobe, *Inorg. Chem.*, 1974, **13**, 1991; (*b*) B. P. Kennedy, R. Gosling and M. L. Tobe, *Inorg. Chem.*, 1977, **16**, 1744; (*c*) R. Gosling and M. L. Tobe, *Inorg. Chim. Acta*, 1980, **42**, 223; (*d*) R. Gosling and M. L. Tobe, *Inorg. Chem.*, 1983, **22**, 1235; (*e*) M. L. Tobe, A. T. Treadgold and L. Cattalini, *J. Chem. Soc., Dalton Trans.*, 1988, 2347.
7 P. L. Goggin, *J. Chem. Soc., Dalton Trans.*, 1974, 1483.
8 BrukerAXS, SMART, Area Detector Control Software, Bruker Analytical X-Ray System, Madison, Wisconsin, USA, 1995.
9 G. M. Sheldrick, SADABS, Program for absorption correction, University of Göttingen, Germany, 1996.
10 BrukerAXS, SAINT, Integration Software, Bruker Analytical X-Ray System, Madison, Wisconsin, USA, 1995.
11 G. M. Sheldrick, SHELXTL5.1, Program for structure solution and least squares refinement, University of Göttingen, Germany, 1998.
12 *Applied Photophysics Bio Sequential SX-17MV Stopped Flow ASVD Spectrofluorimeter, software manual*, Applied Photophysics Ltd., 203/205 Kingston Road, Leatherhead, UK KT22 7PB.
13 R. J. Goodfellow and L. M. Venanzi, *J. Chem. Soc.*, 1965, 7533.
14 (*a*) F. Basolo, J. Chatt, H. B. Gray, R. G. Pearson and B. L. Shaw, *J. Chem. Soc.*, 1961, 2207; (*b*) C. H. Langford and H. B. Gray, *Ligand Substitution Processes*, W. A. Benjamin Inc., New York, 1965.
15 M. R. Plutino, S. Otto, A. Roodt and L. I. Elding, *Inorg. Chem.*, 1999, **38**, 1233.
16 T. P. Cheeseman, A. L. Odell and H. A. Raethel, *Chem. Commun.*, 1968, 1496.
17 See ref. 3*b* for a discussion of the drawbacks of the nucleophilic discrimination approach in acetonitrile.
18 T. G. Appleton and M. A. Bennett, *Inorg. Chem.*, 1978, **17**, 738.
19 (*a*) B. J. Dunne, R. B. Morris and A. G. Orpen, *J. Chem. Soc., Dalton Trans.*, 1991, 653; (*b*) D. S. Marynick, *J. Am. Chem. Soc.*, 1984, **106**, 4064; (*c*) A. G. Orpen and N. G. Connelly, *Organometallics*, 1990, **9**, 1206.
20 As proposed in ref. 19 the P–C σ* orbital is involved in the π acceptor function on phosphorus. See also discussion in ref 3*b*.
21 A. N. Sobolev, V. K. Belsky, N. Yu. Chernikova and F. Yu. Akhmadulina, *J. Organomet. Chem.*, 1983, **244**, 129.